

Mode Selective Stereomutation and Parity Violation in Disulfane Isotopomers H₂S₂, D₂S₂, T₂S₂

by Michael Gottselig, David Luckhaus, Martin Quack*, Jürgen Stohner, and Martin Willeke

Laboratorium für Physikalische Chemie, ETH-Zürich (Zentrum), CH-8092 Zürich

Dedicated to *Edgar Heilbronner* on the occasion of his 80th birthday

We report quantitative calculations of stereomutation tunneling in the disulfane isotopomers H₂S₂, D₂S₂, and T₂S₂, which are chiral in their equilibrium geometry. The quasi-adiabatic channel, quasi-harmonic reaction path Hamiltonian approach used here treats stereomutation including all internal degrees of freedom. The torsional motion is handled as an anharmonic reaction coordinate in detail, whereas all the remaining degrees of freedom are taken into account approximately. We predict how stereomutation is catalyzed or inhibited by excitation of the various vibrational modes. The agreement of our theoretical results with spectroscopic data from the literature on H₂S₂ and D₂S₂ is excellent. We furthermore predict the influence of parity violation on stereomutation as characterized approximately by the ratio ($\Delta E_{pv}/\Delta E_{\pm}$) of the (local or vibrationally averaged) parity violating potential ΔE_{pv} , and the tunneling splittings ΔE_{\pm} in the symmetrical case. This ratio is exceedingly small for the reference molecules H₂O₂ and D₂O₂, and still very small ($2 \cdot 10^{-6} \text{ cm}^{-1}$) for H₂S₂, which, thus, all exhibit essentially parity conservation in the dynamics. However, for D₂S₂ it is *ca.* 0.002, and for T₂S₂ it is *ca.* 1, which seems to be the first case where such intermediate mixing through parity violation is quantitatively predicted for spectroscopically accessible molecules. The consequences for the spectroscopic detection of molecular parity violation are discussed briefly also in relation to other molecules.

1. Introduction. – Geometrical aspects of molecular symmetry have been a key element in discussions of molecular structure and dynamics for some time, with occasionally brilliant presentations of the various facets of this topic [1][2]. At a more fundamental level, the abstract symmetries of the group of the Hamiltonians of physics have been historically known to provide a key to an understanding of the classical and quantum dynamics of physical systems [3]. Such symmetries may be approximate and then can be used as a guiding principle to classify molecular properties ranging from models of electronic structure [4][5] to detailed state-to-state selection rules in chemical reactions [6][7]. A violation of such symmetries and selection rules is then anticipated and understood as providing the structure of various levels of approximation used in our description of nature. However, certain symmetries of physics have an even more fundamental character, being almost accepted *a priori* [8]. The violation of such symmetries, whenever established experimentally, provides deep insight into what is observable or unobservable in nature [9].

The discovery of parity violation in nuclear physics [10][11] and the formulation of electroweak theory [12–14] led to the realization that possible effects from parity violation should also be considered in molecular physics. However, it turns out that the inclusion of parity-violating effective potentials in quantum-chemical calculations is usually not necessary due to their minute size (on the order of $10^{-13 \pm 3} \text{ J mol}^{-1}$ for molecules consisting of lighter elements). An exception are chiral molecules, especially

those with a high barrier for stereomutation, because of their close degeneracy of vibrational tunneling energy levels. Thus, the special situation may arise that the energy difference between the enantiomers of a chiral molecule ΔE_{pv} , which is caused by the parity-violating electroweak interaction, is as large as or even larger than the tunneling splitting in the vibrational ground state. Such a situation is of particular interest, since parity violation becomes dynamically important for the chirality of the molecule [9][15][16].

Indeed, as illustrated in *Fig. 1*, one may distinguish two limiting cases for the structure and dynamics of chiral molecules. In the first case, the tunneling splittings ΔE_{\pm} corresponding to the interconversion of enantiomers are large, much larger than the asymmetric, parity-violating effective potentials corresponding to a hypothetical parity-violating energy difference ΔE_{pv} between the enantiomeric (*R*) and (*S*) equilibrium structures. In this case (*Fig. 1, a*), the molecular eigenfunctions have essentially pure parity (+ or –), being delocalized superpositions of localized ('left' or 'right') λ, ρ structures (see *Fig. 1, a*)

$$\chi_+ = \frac{1}{\sqrt{2}} (\lambda + \rho) \quad (1)$$

$$-\chi_- = \frac{1}{\sqrt{2}} (\lambda - \rho) \quad (2)$$

Recent experimental and theoretical studies show definitively that H_2O_2 [17][18] and aniline-NHD [19] with very low barriers for stereomutation, of *ca.* 5 kJ mol⁻¹, are among these types of molecules. Although such molecules are chiral at their equilibrium geometries, they are not generally considered as ordinary chiral molecules, because the lifetime of chiral structures falls into the femtosecond to picosecond range [17–20]. On the other hand, for typical, stable chiral molecules such as CHFCIBr [21–26], one can estimate that the opposite case applies, with $\Delta E_{\text{pv}} \gg \Delta E_{\pm}$. Then the eigenfunctions are localized with well-defined handedness (λ or ρ) as shown in *Fig. 1, b*

$$\lambda = \frac{1}{\sqrt{2}} (\chi_+ - \chi_-) \quad (3)$$

$$\rho = \frac{1}{\sqrt{2}} (\chi_+ + \chi_-) \quad (4)$$

Only recently, a simultaneous, quantitative theoretical investigation of both parity violation and tunneling splittings has actually shown such a case to apply to S_2Cl_2 [27], which could also be useful for experimental study [15]. Another very interesting case with respect to experiments [16] is an intermediate situation where ΔE_{pv} is on the order of ΔE_{\pm} .

The recent theoretical discovery [28–30] that parity-violating potentials are orders of magnitude larger than previously accepted [31][32] has stimulated new interest in molecular-parity violation, as many more molecules might become dominated by parity violation than hitherto anticipated, and accessible to useful experimental study.

Here, we investigate disulfane isotopomers (X_2S_2 , X = H, D, T; *Fig. 2*). Disulfane isotopomers have a chain structure, and they exhibit C_2 symmetry in their chiral

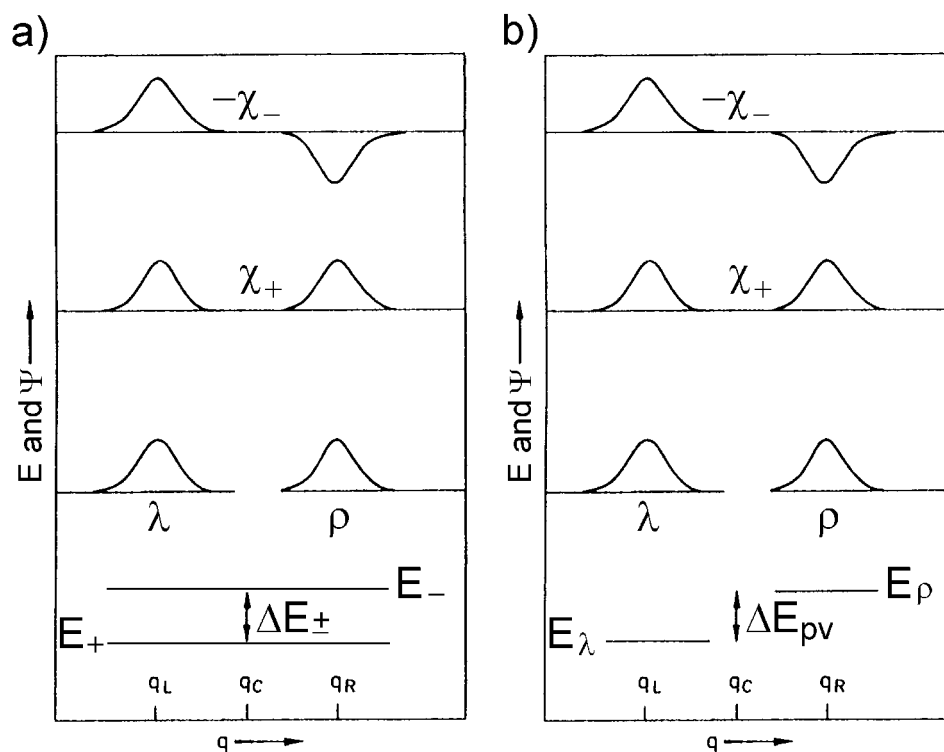


Fig. 1. Quantum-mechanical energy levels (E) and wave functions ($\Psi(=\lambda, \rho, \chi_\pm)$) in the two limiting cases: a) tunneling splitting ΔE_\pm much larger than the parity-violating energy difference ΔE_{pv} , and b) parity-violating energy difference ΔE_{pv} much larger than the tunneling splitting ΔE_\pm .

equilibrium geometry. They are among the simplest prototypes for stereomutation, performing a large amplitude motion – internal rotation, *i.e.*, torsion around the S–S bond. The barriers for stereomutation between the enantiomers of H_2S_2 were determined experimentally [33] and theoretically [34] to be rather high, for the *cis*-barrier *ca.* 2800 cm^{-1} and for the *trans*-barrier *ca.* 2000 cm^{-1} . Accordingly, the torsional tunneling splittings are rather small. For instance, the torsional tunneling splitting in the vibrational ground state (torsional state $\nu_t=0$) was experimentally determined to be *ca.* $2 \cdot 10^{-6} \text{ cm}^{-1}$ [35][36]. Torsional tunneling splittings for higher torsional states have also been determined, either experimentally or theoretically [33][35][37–40]. Moreover, an increased torsional splitting in the millimeter-wave rotational spectra of an excited vibrational state was observed, and possible mechanisms for this increase were discussed [37][41]. For the disulfane isotopomer D_2S_2 , only the torsional tunneling splitting in the torsional state $\nu_t=3$ has been observed. Its value was determined to be $3.3 \cdot 10^{-4} \text{ cm}^{-1}$ [39]. For the first three torsional states of D_2S_2 , there are neither experimental nor calculated torsional tunneling splittings available (except for a preliminary study in our group [42]). To our knowledge, no data have been published for T_2S_2 .

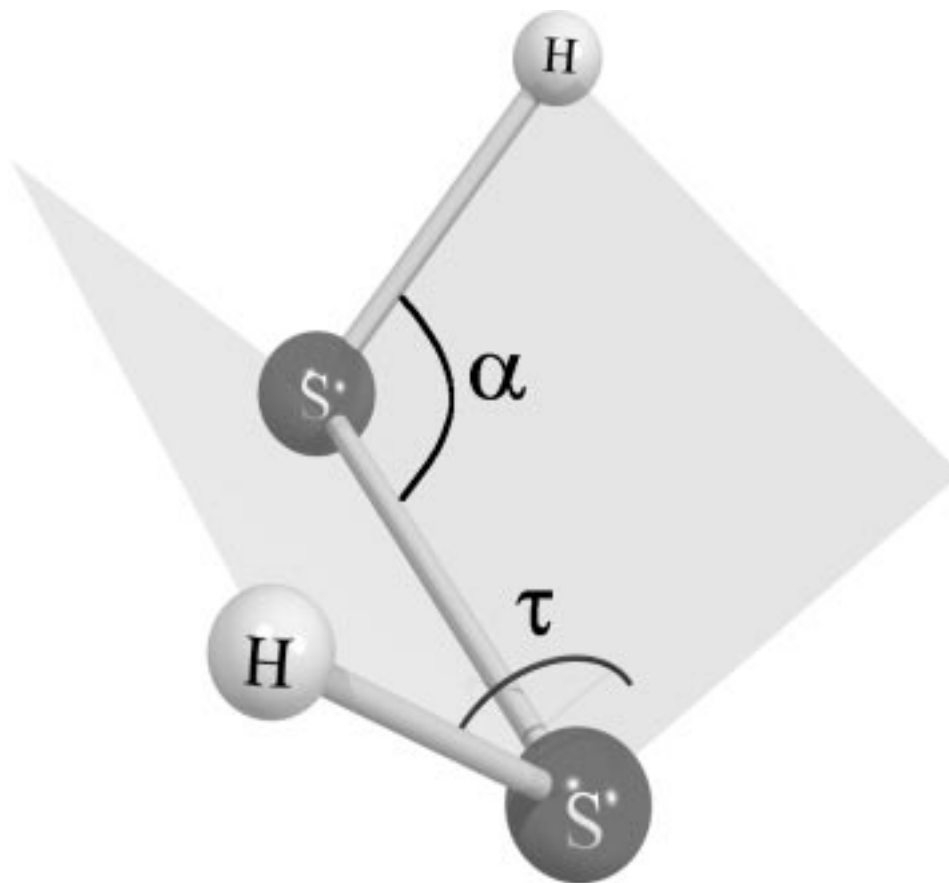


Fig. 2. Chiral C_2 equilibrium structure of the (P)-enantiomer of disulfane obtained employing MP2/6-311 + G(3df,2p) calculations

In this paper, we present our theoretical results for the mode-selective stereomutation tunneling in disulfane isotopomers. The calculations were performed employing the quasiadiabatic channel reaction-path Hamiltonian (RPH) approach [18][19], which has been shown to reproduce well the experimentally observed pure torsional spectrum and mode-specific tunneling, as well as the few known isotope shifts for H_2O_2 , a related molecule. The reaction path Hamiltonian used here is based on earlier work by *Miller, Handy, and Adams* [43], and further related to still earlier adiabatic channel model [44][45] and transition-state-theory treatments [46]. It has also been successfully applied to the inversion dynamics of aniline [19]. Moreover, it has been shown that our harmonic reaction-path Hamiltonian approach gives good agreement with the results of a new fully coupled six-dimensional adiabatic channel approach [18][47]. We compare the torsional tunneling splittings of the disulfane isotopomers with parity-violating potentials [29][34][48][49], including some additional calculations from the present work, and with the corresponding results for hydrogen peroxide [28–30][49]. While the parity-violating energy differences for H_2S_2

and D_2S_2 are small compared with the torsional tunneling-splittings in the vibrational ground state, the parity-violating energy difference for T_2S_2 is of the same order as the torsional splitting. This is, to our knowledge, the first system for which explicit calculations show that $\Delta E_{pv} \approx \Delta E_{\pm}$. Moreover, excitation of the antisymmetric TSS-bending fundamental inhibits the tunneling dynamics, thus possibly inducing the torsional splitting to become smaller than the parity-violation energy difference.

2. Calculations. – The *ab initio* calculations with parity-conserving Hamiltonians were carried out with the *Gaussian 98* quantum-chemistry package [50]. The equilibrium structure and nuclear configurations of disulfane at constrained dihedral angles τ and within the constraints of C_2 symmetry were completely optimized to obtain the parity-conserving torsional potential using second-order *Møller-Plesset* perturbation theory (MP2) [51]. The ‘tight’ *Gaussian 98* convergence criteria were used, and the core electrons were kept frozen. For each nuclear configuration considered, we calculated also the harmonic vibrational frequencies using MP2 analytic second derivatives. For the above-mentioned calculations a 6-311 + *G*(3df, 2p) split-valence basis set was employed. In particular, the torsional potential and the corresponding structures were calculated in steps of 10 degrees. Thus, we calculated the reaction path as a minimum-energy path, which is invariant under isotope substitution. The calculations of parity-violating potentials were carried out according to the MC-LR approach described in [30], making use here of the RPA (random phase approximation) and the Dalton program [69].

The torsional-tunneling dynamics were calculated with the quadiabatic channel-reaction path Hamiltonian treatment described in detail in [18][19]. In brief, it is a modified version of the RPH treatment introduced by *Miller, Handy, and Adams* [43]. We introduce the one-dimensional (RPH) Hamiltonian $\hat{H}_q(\hat{p}, q)$, which depends only upon the reaction coordinate q and its conjugate momentum \hat{p} ,

$$\hat{H}_q = \frac{1}{2} \hat{p} G \hat{p} + u(q) + V_e(q) \quad (5)$$

V_e is the electronic potential along the minimum-energy path, the momentum operator \hat{p} has its usual definition

$$\hat{p} = -i\hbar \frac{\partial}{\partial q} \quad (6)$$

The effective inverse reduced mass G is obtained by pointwise inversion according to

$$G^{-1}(q) = \sum_{i=1}^N \frac{\partial \mathbf{a}_i(q)}{\partial q} \frac{\partial \mathbf{a}_i(q)}{\partial q} \quad (7)$$

with the reference geometry $\mathbf{a}_i(q)$ in terms of the mass-weighted cartesian-coordinate vectors of the atoms i . $u(q)$ is the pseudo potential. The complete vibrational Hamiltonian is given by

$$\hat{H}(\hat{p}, q, \{\hat{P}_k, Q_k\}) = \hat{H}_Q(\{\hat{P}_k, Q_k\}; q) + \hat{H}_q(\hat{p}, q) \quad (8)$$

where the first part depends on the ‘fast’ $3N - 7$ mass weighted normal coordinates Q_k and their conjugate momenta \hat{P}_k , and parametrically upon q , the ‘slow’ reaction-channel coordinate. The eigenfunctions in the quasi-harmonic-quasi-adiabatic channel approach are given by the products

$$\Psi_m^n(\mathbf{Q}, q) = \chi_m^n(q) \varphi_n(\mathbf{Q}; q). \quad (9)$$

$$\hat{H}_Q \varphi_n(\mathbf{Q}; q) = \varepsilon_n(q) \varphi_n(\mathbf{Q}; q) \quad (10)$$

The $\varphi_n(\mathbf{Q}; q)$ are harmonic-oscillator eigenfunctions. The $\chi_m^n(q)$ are associated with the adiabatic channel n

$$(\varepsilon_n(q) + \langle \varphi_n | \hat{H}_q | \varphi_n \rangle - E_m^n) \chi_m^n(q) = 0. \quad (11)$$

Eqn. 11 is solved numerically in a discrete variable representation (DVR). Avoided crossings of adiabatic channels are removed in the modified approach by a systematic deperturbation by means of 2×2 diabatic rotations in normal coordinate space. For details, we refer to [18][19]. The existing computer program package from [18][19] was modified to allow for much higher numerical precision. We use 128-bit word length (quadruple precision) for a floating-point number. However, the originally calculated *ab initio* values for the electronic potential energies, force fields, and cartesian coordinates were by far not represented with a comparable precision. This causes high-frequency artificial noise. It furthermore leads to a very slow numerical convergence in the calculation of extremely small tunneling splittings as a function of increasing number of grid points, because each added grid point possibly adds even higher-frequency noise. To avoid these numerical problems, the effective potential $V(\tau(q)) = V_e(q) + u(q)$, all harmonic transition wavenumbers functions $\omega_i(\tau(q))$, and $G(\tau(q))$ were fitted to a *Fourier* series up to 16th-even-order, which acts as a filter for the numerical noise

$$F(\tau(q)) = F_0 + \sum_{i=2, \text{even}}^{16} F_i \times \cos(\pi i \tau(q)/360). \quad (12)$$

For symmetry reasons, all expansion terms F_i with an odd index i are zero. This expansion was found to be sufficient. The root-mean-square deviations were lower than one part per thousand with respect to the maximum value of the fitted function. It is expected that these deviations have a negligible influence on our calculations.

While the fully anharmonic quasiadiabatic channel approach should be fairly accurate, also with respect to absolute energies except for local resonances, and can be implemented when a full potential surface is available, for instance, with the quasi-adiabatic-channel quantum Monte Carlo or DVR techniques [52][53], the present approach contains substantial further approximations (most importantly the quasiharmonic approximation for the $3N - 7$ normal modes). Thus, the absolute vibration-torsion energies are not expected to be accurate. It has been demonstrated before, however, for the rather similar example H_2O_2 , that the stereomutation tunneling is well approximated by the present approach. For H_2O_2 , such a validation was possible by comparison with fully six-dimensional, ‘exact’ DVR calculations [18][47], as a

complete six-dimensional potential hypersurface is available [17]. The approximate and exact tunneling splittings were almost identical for the case, when there are no resonances. This gives us confidence to expect similar accuracy for H_2S_2 , where a full six-dimensional hypersurface is not yet available, and exact six-dimensional calculations cannot be carried out for this reason. Indeed, the major advantage of the quasiadiabatic channel RPH approaches consists in the possibility of obtaining fairly accurate results with full-dimensional dynamics in cases where a global electronic potential hypersurface is not available. Some initial calculations [42] were carried out with a simple one-dimensional flexible model Hamiltonian [54] and an effective, adjusted potential for the torsional motion only [42]. They will be given here for comparison.

3. Results and Discussion. – *Table 1* compares the symmetric tunneling components (A^+) of calculated fundamental transition wavenumbers for disulfane and its isotopomers with the experimental results for the band centers and with the harmonic wavenumbers from *ab initio* theory. One finds the typical deviations that are due to fundamentals being different from harmonic frequencies because of anharmonicity and due to the *ab initio* error in harmonic frequencies. However, the torsional transition wavenumbers agree very well. This is to be expected, since the RPH approach treats the torsional vibration anharmonically. For T_2S_2 , there exist, to our knowledge, no experimental data. Moreover, in *Table 2* it is shown that the experimental r_e -structure agrees reasonably well with our calculated MP2/6-311 + G(3df,2p) structure.

Table 3 displays the calculated results for the torsional tunneling splittings of disulfane in the first six pure torsional states compared with experimental and other

Table 1. *Calculated and Experimental Wavenumbers for the Vibrational Modes of H_2S_2 , D_2S_2 , and T_2S_2 .* All values are given in cm^{-1} . In the following assignments s refers to a stretching and b to a bending mode: $\nu_1 = sym. s(SX)$, $\nu_2 = sym. b(SSX)$, $\nu_3 = s(SS)$, $\nu_4 = torsion$, $\nu_5 = asym. s(SX)$, $\nu_6 = asym. b(SSX)$ where $X = H, D, T$

	H_2S_2				D_2S_2		T_2S_2
	Exper. ^{a)}	RPH ^{b)}	Calc. ^{c)}	Calc. ^{d)}	Exper. ^{c)}	RPH ^{b)}	RPH ^{b)}
ν_1	2555.8	2728.6	2726.6	2657.3	–	1959.8	1625.5
ν_2	883	911.4	912.6	886.9	–	659.8	553.8
ν_3	515.9	539.1	537.4	500.8	–	537.1	532.3
ν_4	417.5	424.8	450.7	412.9	306	311.5	260.8
ν_5	2558.6	2731.1	2729.2	2658.3	1863	1961.5	1626.7
ν_6	882	905.81	909.9	882.3	646.4	653.7	545.6

^{a)} Experimental gas-phase data from [55–58]. ^{b)} Quasiharmonic RPH calculations, this work. ^{c)} *Ab initio* harmonic wavenumbers from this work MP2/6-311 + G(3df,2p). ^{d)} *Ab initio* harmonic wavenumbers from [59] (CCSD(T)/6-311 ++ G(2d,2p)). ^{e)} Experimental gas-phase data from [57].

Table 2. *Experimental and Ab Initio Equilibrium Geometry of H_2S_2*

Parameter	Exper. [60]	MP4/cc-pVTZ [61]	MP2/6-311 + G(3df,2p), This work
$r_{SS}/\text{Å}$	2.0564(1)	2.083	2.053
$r_{SH}/\text{Å}$	1.3418(2)	1.344	1.338
$\alpha_{SSH}/^\circ$	97.91(5)	97.71	98.19
$\tau_{HSSH}/^\circ$	90.40(10)	90.55	90.78

Table 3. *Torsional Tunneling Splittings* ($\tilde{\nu}(A^-) - \tilde{\nu}(A^+)$) of H_2S_2 for Pure Torsional States $\tilde{\nu} = \nu_t \cdot \nu_t$. All values are given in cm^{-1}

ν_t	Exper.	Note	RPH ^{a)}	Calc. ^{b)}	Calc. ^{c)}	Fit ^{d)}	1d ^{e)}
0	$1.935 \cdot 10^{-6}$ $2.502 \cdot 10^{-6}$	^{f)} ^{h)}	$1.985 \cdot 10^{-6}$	– ^{g)}	$1.115 \cdot 10^{-5}$	– ^{g)}	$2.616 \cdot 10^{-6}$
1	$2.667 \cdot 10^{-4}$	ⁱ⁾	$2.245 \cdot 10^{-4}$	$2 \cdot 10^{-4}$	$3.87 \cdot 10^{-4}$	$2.50 \cdot 10^{-4}$	$2.783 \cdot 10^{-4}$
2	$1.2547 \cdot 10^{-2}$ $1.2672 \cdot 10^{-2}$	^{j)} ^{k)}	$1.112 \cdot 10^{-2}$	$0.83 \cdot 10^{-2}$	$1.91 \cdot 10^{-2}$	$1.26 \cdot 10^{-2}$	$1.333 \cdot 10^{-2}$
3	$3.550 \cdot 10^{-1}$	^{k)}	$3.134 \cdot 10^{-1}$	–	$5.6 \cdot 10^{-1}$	$3.69 \cdot 10^{-1}$	$3.69 \cdot 10^{-1}$
4	–		5.319	–	9.9	6.49	6.15
5	–		44.815	–	70.1	–	–

^{a)} RPH Calculations, this work. ^{b)} Variational calculations [38]. ^{c)} Variational calculations [40]. ^{d)} Determined with an effective potential adjusted to the experimental tunneling splittings for $\nu_t=0, 1, 2$ [39]. ^{e)} One-dimensional flexible model [42] with adjusted potential from [33], this work. ^{f)} From millimeter-wave data [35][37]. ^{g)} Within their numerical precision determined to be zero. ^{h)} From saturation spectroscopy [36]. ⁱ⁾ From millimeter-wave data [37]. ^{j)} From millimeter-wave data [33]. ^{k)} From IR data [33].

previously published data. Our RPH results agree very well with experiment, particularly in view of the absence of any adjustment to experiment. This holds even for the very small splitting in the torsional ground state. Other *ab initio* methods yielded either a ‘zero’ value (due to insufficient numerical precision [38]) or a value one order of magnitude too large [40]. Moreover, our *ab initio* values agree well with those that were determined with an effective torsional potential, which had been adjusted to the experimental torsional splittings for the first three torsional states ($\nu_t=0, 1, 2$). The predictions obtained from the latter effective potential for the tunneling splittings in the torsional states $\nu_t=3, 4$ agree with the results of our RPH calculations. The torsional energy levels for the pure torsional states up to the *trans*-barrier to stereomutation are shown in *Fig. 3*.

For D_2S_2 (see *Table 4*), only the $\nu_t=3$ tunneling splitting is experimentally known. The torsional tunneling splitting that we obtain *ab initio* agrees approximately with the experimental result. Altogether, our calculated torsional tunneling splittings for H_2S_2 and D_2S_2 agree well with experiment. The calculated splittings are always smaller (*ca.* 11–21%, if one does not take the early experimental value of $1.935 \cdot 10^{-6} cm^{-1}$ into account, which we would reproduce within < 3%). Thus, we expect our predictions for the pure torsional tunneling splittings for D_2S_2 in the torsional states $\nu_t=0, 1, 2$, and 5 as well as for T_2S_2 (see *Table 4*) to be good estimates of the true values. This is also supported by the relatively good comparison of our results with the simple, one-dimensional adjusted model potential.

A question of considerable current interest in chemical-reaction dynamics concerns vibrational-mode selectivity [62–64]. As we have discussed for the case of H_2O_2 [18], the question arises in this context, whether excitation of certain, nontorsional vibrational modes promotes (‘catalyzes’) or inhibits the prototype reaction of stereomutation. The results of our investigation of the mode selectivity of the tunneling process in disulfane isotopomers are shown in *Table 5*. Our comparison with experimental data is, in this case, limited, since only the enhanced splitting in the first excited S–S stretching state of H_2S_2 has been observed so far. Moreover, this particular

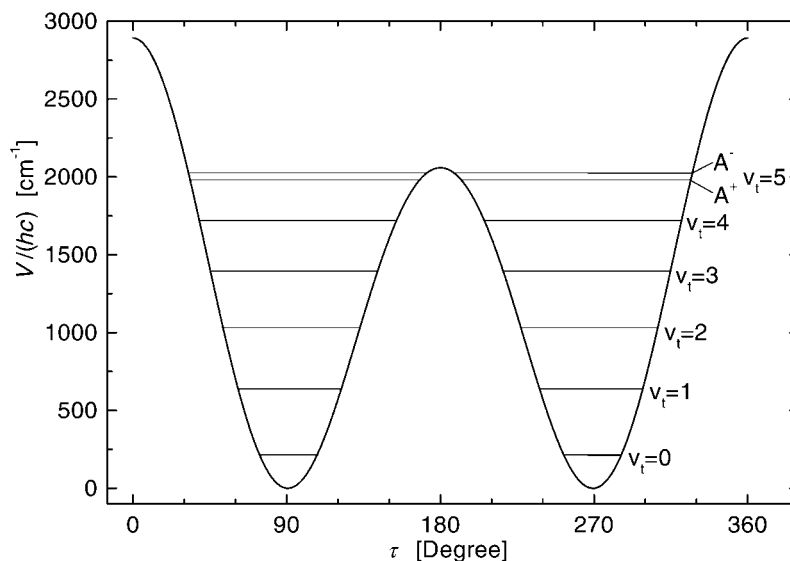


Fig. 3. Parity-conserving torsional potential $V(\tau)$ plotted as a function of the dihedral angle τ and torsional energy levels for different torsional states $v_t = 1 \dots 5$ of H_2S_2 , which have been superimposed on the potential. Only the torsional splitting ($\tilde{\nu}(A^-) - \tilde{\nu}(A^+)$) for the $v_t = 5$ level is large enough to be depicted (see Table 2)

Table 4. Torsional Tunneling Splittings ($\tilde{\nu}(A^-) - \tilde{\nu}(A^+)$) of D_2S_2 and T_2S_2 for pure torsional states $\tilde{\nu} = v_t \cdot \nu_t$. All values are given in cm^{-1}

v_t	D_2S_2			T_2S_2		
	Exper. [38]	RPH ^{a)}	1d ^{b)}	Fit. ^{c)}	RPH ^{a)}	1d ^{b)}
0	–	$4.827 \cdot 10^{-10}$	$6.014 \cdot 10^{-10}$	– ^{d)}	$1.151 \cdot 10^{-12}$	$1.476 \cdot 10^{-12}$
1	–	$7.805 \cdot 10^{-8}$	$9.43 \cdot 10^{-8}$	– ^{d)}	$2.270 \cdot 10^{-10}$	$2.835 \cdot 10^{-10}$
2	–	$5.833 \cdot 10^{-6}$	$6.88 \cdot 10^{-6}$	– ^{d)}	$2.107 \cdot 10^{-8}$	$2.565 \cdot 10^{-8}$
3	$3.33 \cdot 10^{-4}$	$2.660 \cdot 10^{-4}$	$3.07 \cdot 10^{-4}$	$1.80 \cdot 10^{-4}$	$1.220 \cdot 10^{-6}$	$1.447 \cdot 10^{-6}$
4	–	$8.198 \cdot 10^{-3}$	$9.28 \cdot 10^{-3}$	$5.76 \cdot 10^{-3}$	$4.915 \cdot 10^{-5}$	$5.675 \cdot 10^{-5}$
5	–	$1.776 \cdot 10^{-1}$	–	–	$1.451 \cdot 10^{-3}$	$1.629 \cdot 10^{-3}$

^{a)} RPH Calculations, this work. ^{b)} This work with one-dimensional model potential adjusted to data for H_2S_2 (Table 3). ^{c)} Determined with an effective potential adjusted to the experimental tunneling splittings of H_2S_2 for $v_t = 0, 1, 2$ [39]. ^{d)} Zero within numerical uncertainties.

splitting has been interpreted to be perturbed by an anharmonic resonance coupling between the first excited S–S stretching state and the manifold of excited torsional states with torsional splittings much larger than 1.0 MHz [36] [41]. In such a case, where anharmonic resonance effects markedly shift vibrationally excited levels, the quasi-adiabatic harmonic approach necessarily fails. This explains that our theoretical result is approximately seven times smaller than the experimental splitting [41]. However, our result supports the assumption that the unperturbed, zero-order torsional tunneling splitting in the first excited S–S stretching vibration in H_2S_2 is about equal to the ground-state torsional tunneling splitting [36] [41].

Table 5. *Mode-Specific Stereomutation Tunneling of H₂S₂, D₂S₂, and T₂S₂: Torsional Tunneling Splittings $\Delta\tilde{\nu}_i = (\tilde{\nu}(A^-) - \tilde{\nu}(A^+))$ for Fundamental Excitations $\tilde{\nu}_i$*

	H ₂ S ₂ $\Delta\tilde{\nu}_i/10^{-6}$ cm ⁻¹			D ₂ S ₂ $\Delta\tilde{\nu}_i/10^{-10}$ cm ⁻¹		T ₂ S ₂ $\Delta\tilde{\nu}_i/10^{-12}$ cm ⁻¹
	Exper.	RPH ^{a)}	Calc. ^{b)}	Calc. [41]	RPH ^{a)}	RPH ^{a)}
ν_0	1.935 ^{c)} 2.502 [35]	1.985	11.15	–	4.827	1.151
ν_1	–	1.613	–300	–	3.898	0.924
ν_2	–	1.001	1400	–	12.747	3.283
ν_3	14.67 ^{d)} ^{e)} 16.7 ^{e)}	2.051	47	34.2	5.299	1.300
ν_5	–	1.570	18000	–	3.821	0.917
ν_6	–	4.768	400	–	2.095	0.465

^{a)} RPH Calculations, this work. ^{b)} Variational calculations [40]. ^{c)} From millimeter-wave data [37]. ^{d)} From millimeter-wave data [41]. ^{e)} Assumed to be perturbed by anharmonic resonance [37][41].

Overall, one finds that ν_3 appears to be an ineffective mode, the symmetric bending mode ν_2 is a rather strongly promoting mode, whereas the asymmetric bending mode ν_6 is a rather strongly inhibiting mode for D₂S₂ and T₂S₂. For H₂S₂, ν_2 is an inhibiting and ν_6 a promoting mode. The two HS stretching modes are weakly inhibiting modes. This remains true for the isotopomers. Furthermore, this overall picture is also not too different from that for H₂O₂ [18], where the effects are generally more pronounced, and the splittings are much larger. *Figs. 4* and *5* provide a convenient graphical survey of these results.

Finally, it is of interest to compare the tunneling splittings with calculations for the parity-violating energy difference ΔE_{pv} , which we take here as the difference of parity-violating potentials (or total energies) at the assumed or calculated equilibrium geometries of the enantiomers

$$\Delta E_{\text{pv}} \approx E_{\text{pv}}(M) - E_{\text{pv}}(P) \quad (13)$$

$$\approx 2E_{\text{pv}}(M). \quad (14)$$

As there is a rather strong dependence of E_{pv} upon torsional angle [29][30][34], this single number is not quite sufficient for complete characterization. For the present purpose of an overall order of magnitude study, it should be sufficient, however. This conclusion is supported by the more accurate calculation of torsional-energy levels including an antisymmetric parity-violating effective potential.

Table 6 summarizes the results for ΔE_{pv} for H₂O₂ and H₂S₂ as obtained from previous and present calculations. As defined here, the sign is different for H₂O₂ and H₂S₂, that is, for H₂O₂, the potential is lower for the (*M*)-enantiomer than for the (*P*)-enantiomer near the equilibrium geometry (τ_e), whereas, for H₂S₂, the potential is lower for the (*P*)-enantiomer than for the (*M*)-enantiomer near (τ_e). *Table 6* shows that, for H₂O₂, the early results for $|E_{\text{pv}}|$ are lower by about two orders of magnitude than all current results, as first established in [28]. For H₂S₂, the corresponding increase is still more than an order of magnitude. For a critical discussion of the smaller differences in recent calculations, we refer to [30][34]. We should note that, because of the relatively strong dependence of ΔE_{pv} upon geometry, a global comparison should

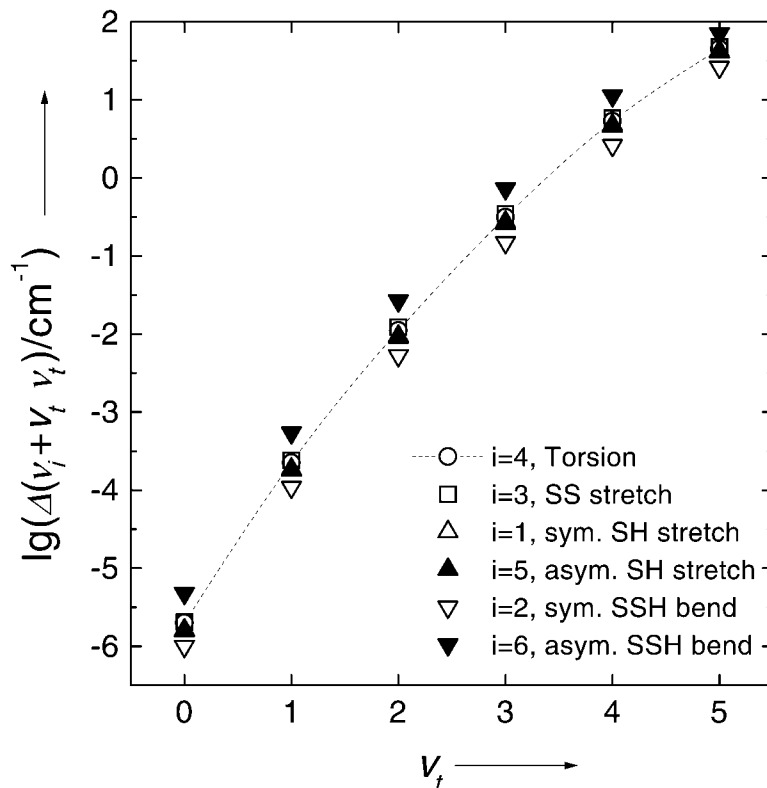


Fig. 4. Mode-specific stereomutation tunneling of H_2S_2 : logarithmic plot of the torsional tunneling splittings $\Delta(v_i + v_t \cdot v_i)$ for the singly excited fundamentals v_i in dependence of the torsional state v_t with respect to the lowest corresponding A^+ fundamental level

really be made on the basis of comparing the behavior of E_{pv} as a function of geometry, including all degrees of freedom, but this aspect is dealt with separately [49]. Suffice to say that, of course, results from different calculations on ΔE_{pv} are only comparable, when they refer to exactly the same geometry. We give in Table 6 results for two sets of geometry for H_2S_2 .

Here, we should discuss the relative magnitude of $|\Delta E_{pv}|$ and $|\Delta E_{\pm}|$ for the various molecules. For convenience we summarize these data in Table 7 for survey, presenting the rounded values for ΔE_{\pm} just for the vibrational ground state and a rounded 'current best estimate' for $|\Delta E_{pv}|$. Because the hydrogen-isotope nuclei do not contribute much to the parity-violating potential due to the low electroweak charges compared to oxygen and sulfur [29][30], we have inserted the same value of $|\Delta E_{pv}|$ for all isotopomers. The $|\Delta E_{pv}|$ of the D and T isotopomers were calculated with a small basis for confirmation of this result. The changes due to the different effective geometries are presumably as large as those arising from the changes in electroweak charges. For H_2O_2 and D_2O_2 , the tunneling splittings are so much larger than the parity-violating potentials that, for all practical purposes, the observable

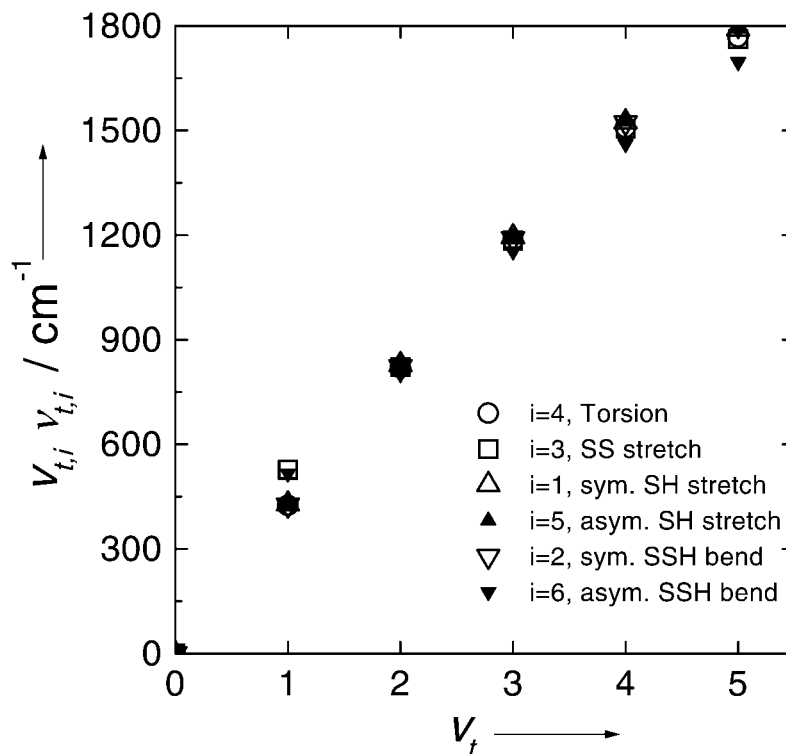


Fig. 5. Mode-specific stereomutation tunneling of H_2S_2 : torsional energy levels for the singly excited fundamentals v_i relative to the energy of the lowest corresponding torsional level

energy eigenstates of H_2O_2 can be considered to have well-defined parity (and no well-defined chirality). The average mixing of the wrong parity into these ‘pure parity’ levels is of the order of $x = (|\Delta E_{\text{pv}}| / |\Delta E_{\pm}|)^2 \approx 10^{-28}$ in this case, which will hardly be detectable by any of the currently available or proposed spectroscopic techniques. While the situation is still about similar for H_2S_2 ($x \approx 10^{-13}$) this changes somewhat for D_2S_2 , where a mixing of $x \approx 10^{-6}$ (and more for some excited vibrational levels) might become detectable with advanced spectroscopic techniques, although the levels will show essentially pure parity (and no chirality). For T_2S_2 $|\Delta E_{\text{pv}}|$ and $|\Delta E_{\pm}|$ are about equal, leading thus to very substantial mixing of the levels of different parity, a prediction that is independent of the precise level of accuracy of the present calculations. To our knowledge, T_2S_2 is the first molecule for which this range of relative order of magnitude for $|E_{\pm}|$ and $|\Delta E_{\text{pv}}|$ has been explored by quantitative theory. Because $|\Delta E_{\text{pv}}|$ depends so strongly upon geometry, the comparison of $|E_{\text{pv}}|$ and $|\Delta E_{\pm}|$ in the first columns of Table 7 gives only a qualitative or at best semiquantitative estimate of the effect of parity-violating potentials on the torsional energy levels and wave functions. As another approximation to estimate the effects from parity violation, we have calculated the changes in positions of the lowest-torsional-energy levels when calculating these with an effective torsional potential including parity violation (over

Table 6. Parity-Violating Energy Difference $\Delta E_{pv} = E_{pv}(M) - E_{pv}(P)$ for H_2S_2 and H_2O_2

Molecule	Method	$\Delta E_{pv}/10^{-13} \text{ cm}^{-1}$
$H_2O_2^a)$	6-31G [32]	-0.003
	CIS/6-31G [28][29] [34]	-0.50
	TDA/6-31G [65]	-0.70
	DHF [48]	-0.37
	CASSCF-LR/cc-pVTZ [30]	-0.34
H_2S_2	4-31G [32] ^{b)}	0.20
	TDA/4-31G (scaled 74.9%) [65] ^{b)}	12.0
	RPA/extended (scaled 74.9%) [65] ^{b)}	19.4
	CIS-RHF/6-31G [29][34] ^{b)}	15.1
	CIS-RHF/D95** [29][34] ^{b)}	16.3
	CIS-RHF/6-311G** [29][34] ^{b)}	18.8
	RPA/6-31G (this work) ^{b)}	14.3
	RPA/cc-pVDZ (this work) ^{b)}	16.5
	RPA/cc-pVTZ (this work) ^{b)}	18.5
	RPA/aug-cc-pVTZ (this work) ^{b)}	18.7
	DHF [48] ^{b)}	28.0
	RPA/cc-pVDZ (this work) ^{c)}	5.7
	RPA/cc-pVTZ (this work) ^{c)}	6.6
RPA/aug-cc-pVTZ (this work) ^{c)}	7.0	

^{a)} Using the geometry: $r_{OO} = 1.49 \text{ \AA}$, $r_{OH} = 0.97 \text{ \AA}$, $\alpha_{OOH} = 100.0^\circ$, and $\tau_{HOOH} = 90.0^\circ$. ^{b)} Using the geometry: $r_{SS} = 2.055 \text{ \AA}$, $r_{SH} = 1.352 \text{ \AA}$, $\alpha_{SSH} = 92.0^\circ$, and $\tau_{HSSH} = 90.0^\circ$. ^{c)} Employing the MP2/6-311 + G(3df,2p) equilibrium structure shown in *Table 2*.

Table 7. Comparison of $|\Delta E_{pv}|$ and $|\Delta E_{\pm}|$ for Various Molecules

Molecule	$ \Delta E_{pv} /\text{cm}^{-1}$	$ \Delta E_{\pm} /\text{cm}^{-1}$	$y = \frac{\Delta E_{0,1}^{pv} - \Delta E_{\pm}}{\Delta E_{\pm}}$
H_2O_2	$4 \cdot 10^{-14}$	11	–
D_2O_2	$4 \cdot 10^{-14}$	2	–
H_2S_2	$1 \cdot 10^{-12}$	$2 \cdot 10^{-6}$	$4.5 \cdot 10^{-13}$
D_2S_2	$1 \cdot 10^{-12}$	$5 \cdot 10^{-10}$	$7.6 \cdot 10^{-6}$
T_2S_2	$1 \cdot 10^{-12}$	$1 \cdot 10^{-12}$	0.91

the full range of torsion angles) as compared to the symmetric potential. These results are shown in the last column of *Table 7* in the form of the ratio of splittings of the lowest two levels calculated including parity violation ($\Delta E_{0,1}^{pv}$) and without parity violation (*i.e.*, $\Delta E_{0,1} = \Delta E_{\pm}$) by means of the expression

$$y = \frac{\Delta E_{0,1}^{pv} - \Delta E_{\pm}}{\Delta E_{\pm}} \quad (15)$$

Further, similar results were obtained using a simple one-dimensional model potential including parity violation. The various types of results agree in their order of magnitude estimate for the effect of parity violation, and further improvements would require a full-dimensional treatment for parity-violating potential hypersurfaces [49]. It must be understood in discussing such calculations including parity-violating potentials that these must not be naively considered as simple additions to the *Born-Oppenheimer* potential governing the nuclear motion within the molecule. Indeed,

non-*Born-Oppenheimer* effects, radiative effects, and related corrections would be all much larger than the parity-violating potentials. Nevertheless, the latter can be introduced as effective potentials into the dynamics, because their different symmetry allows them to be isolated from all other corrections in the perturbation theory (see also the discussion in [29]).

4. Conclusions and Outlook. – In combination with *ab initio* calculations, the quasi-adiabatic channel quasi-harmonic reaction-path Hamiltonian approach allows us to make quantitative predictions of good accuracy for the stereomutation tunneling splittings and rates of the series of chalcogene derivatives of the form X_2Y_2 , which are chiral in their equilibrium geometries. Although the stereomutation process in these compounds is dominated by the torsional motion, the theoretical approach treats the problem in all six internal degrees of freedom, where the influence of the other, nontorsional vibrational modes is taken into account approximately. This allows us to demonstrate mode-selective catalysis and inhibition of stereomutation by the various vibrational modes in H_2S_2 , D_2S_2 , and T_2S_2 . Where available for comparison, experimental data agree well with our theoretical results. Our work provides furthermore a number of predictions for spectroscopically accessible levels.

At a more fundamental level, our calculations of the very small tunneling splittings predicted for D_2S_2 and T_2S_2 allow an interesting comparison with parity-violating potentials. It is found that, with the new order of magnitude of parity violation discovered about 5 years ago [28], and with the present calculations of both parity violation and tunneling splittings, these two isotopomers are potentially useful candidates for the spectroscopic investigation of parity violation. Indeed, for D_2S_2 the parity-violating mixing of spectroscopic levels, while still weak (10^{-5}), might be detectable by spectroscopic techniques, and we thus propose to reinvestigate the spectroscopy of this easily accessible molecule under this aspect. For T_2S_2 , the mixing is predicted to be essentially complete with $|\Delta E_{pv}| \approx |\Delta E_{\pm}|$ and large relative effects of the parity-violating potential on the calculated positions of the lowest torsional levels. These are to our knowledge the first quantitative predictions of this type. The present findings can be extended to X_2Y_2 chalcogenic molecules, where parity violation actually dominates chirality [27]. One obvious set of candidates is the series of isotopomers H_2Se_2 , D_2Se_2 , and T_2Se_2 , as well as the Te compounds (parity violation, but no tunneling splittings, has been studied for H_2Te_2 with relativistic *Hückel* techniques [66] and more recently *Dirac Fock* techniques [48]). Our approach to multidimensional tunneling can treat such systems easily. However, they are neither handled easily by experiment nor is the underlying many-electron relativistic theory well under control. The other option is to use substituted molecules of the type S_2Cl_2 , which is under current study in our laboratory [27], and where parity violation, indeed, dominates tunneling. Another obvious extension of our work concerns the investigation of biomolecules [67][68].

We have received stimulus and encouragement in our investigations through several discussions on symmetry with *Edgar Heilbronner*, to whom this paper is thus justly dedicated. Help from and discussions with *Robert Berger*, *Benjamin Fehrensén*, *Rolf Meyer*, *Achim Sieben*, and *Ioannis Thanopoulos* are gratefully acknowledged. Our work is supported financially by the *Swiss National Science Foundation* and *ETH-Zürich* (including CSCS and C4 projects).

REFERENCES

- [1] E. Heilbronner, J. D. Dunitz, 'Reflections on Symmetry', Verlag Helvetica Chimica Acta, Basel, and VCH, Weinheim, 1993.
- [2] E. Heilbronner, 'Über die Symmetrie in der Chemie', Panta Rhei Book, Verlag Hans Erni Stiftung Luzern, Switzerland, 1981.
- [3] K. Mainzer, 'Symmetrien der Natur', de Gruyter, Berlin, 1988.
- [4] E. Heilbronner, H. Bock, 'Das HMO-Modell und seine Anwendung', VCH, Weinheim, 1968.
- [5] R. B. Woodward, R. Hoffmann, 'The Conservation of Orbital Symmetry', VCH, Weinheim, 1970.
- [6] M. Quack, *Mol. Phys.* **1977**, *34*, 377.
- [7] M. Cordonnier, D. Uy, R. M. Dickson, K. E. Kerr, Y. Zhang, T. Oka, *J. Chem. Phys.* **2000**, *113*, 3181; D. Uy, M. Cordonnier, T. Oka, *Phys. Rev. Lett.* **1997**, *78*, 3844.
- [8] I. Kant, 'Kritik der reinen Vernunft'; see also the earlier discussion 'Von dem ersten Grunde des Unterschieds der Gegenden im Raume', I. Kant, Werke, Vorkritische Schriften, Insel Verlag, Wiesbaden 1960.
- [9] M. Quack, *Nova Acta Leopoldina NF* **1999**, *81*, 137.
- [10] T. D. Lee, C. N. Yang, *Phys. Rev.* **1956**, *104*, 254.
- [11] C. S. Wu, E. Ambler, R. W. Hayward, D. D. Hoppes, R. P. Hudson, *Phys. Rev.* **1957**, *105*, 1413.
- [12] S. L. Glashow, *Nucl. Phys.* **1961**, *22*, 579.
- [13] S. Weinberg, *Phys. Rev. Lett.* **1967**, *19*, 1264.
- [14] A. Salam, in 'Proc. 8th Nobel Symposium on Elementary Particle Theory: Weak and Electromagnetic Interactions', Ed. N. Svartholm, Amkvist and Wiksell, 1968, pp. 367–377.
- [15] M. Quack, *Chem. Phys. Lett.* **1986**, *132*, 147.
- [16] M. Quack, *Angew. Chem.* **1989**, *101*, 588, *Angew. Chem., Int. Ed.* **1989**, *28*, 571.
- [17] B. Kuhn, T. R. Rizzo, D. Luckhaus, M. Quack, M. A. Suhm, *J. Chem. Phys.* **1999**, *111*, 2565.
- [18] B. Fehrensens, D. Luckhaus, M. Quack, *Chem. Phys. Lett.* **1999**, *300*, 312.
- [19] B. Fehrensens, D. Luckhaus, M. Quack, *Z. Phys. Chem. (Oldenbourg)* **1999**, *209*, 1.
- [20] B. Fehrensens, M. Hippler, M. Quack, *Chem. Phys. Lett.* **1998**, *298*, 320.
- [21] A. Beil, D. Luckhaus, R. Marquardt, M. Quack, *J. Chem. Soc., Faraday Trans.* **1994**, *99*, 49.
- [22] A. Bauder, A. Beil, D. Luckhaus, F. Müller, M. Quack, *J. Chem. Phys.* **1997**, *106*, 7558.
- [23] M. Quack, J. Stohner, *Phys. Rev. Lett.* **2000**, *84*, 3807; J. Stohner, A. Beil, H. Hollenstein, O. Monti, M. Quack, in '37th IUPAC Congress and 27th GDCh Meeting', Berlin, Germany, August 14–19, 1999, *Frontiers in Chemistry: Molecular Basis of the Life Sciences*, 525.
- [24] M. Quack, J. Stohner, *Z. Phys. Chem. (Oldenbourg)* **2000**, *214*, 675.
- [25] M. Quack, J. Stohner, *Chirality* **2001**, in press.
- [26] C. Daussey, T. Marrel, A. Amy-Klein, C. T. Nguyen, C. J. Borde, C. Chardonnet, *Phys. Rev. Lett.* **1999**, *83*, 1554.
- [27] R. Berger, M. Gottselig, M. Quack, M. Willeke, to be published.
- [28] A. Bakasov, T.-K. Ha, M. Quack, in 'Chemical Evolution: Physics of the Origin and Evolution of Life', Eds. J. Chela-Flores, F. Raulin, Kluwer Academic Publisher, Netherlands, 1996, pp. 287–296.
- [29] A. Bakasov, T.-K. Ha, M. Quack, *J. Chem. Phys.* **1998**, *109*, 7263.
- [30] R. Berger, M. Quack, *J. Chem. Phys.* **2000**, *112*, 3148.
- [31] R. A. Hegstrom, D. W. Rein, P. G. H. Sandars, *J. Chem. Phys.* **1980**, *73*, 2329.
- [32] S. Mason, G. Tranter, *Mol. Phys.* **1984**, *53*, 1091.
- [33] S. Urban, E. Herbst, P. Mittler, G. Winnewisser, K. M. T. Yamada, M. Winnewisser, *J. Mol. Spectrosc.* **1989**, *137*, 327.
- [34] A. Bakasov, M. Quack, *Chem. Phys. Lett.* **1999**, *303*, 547.
- [35] E. Herbst, G. Winnewisser, *Chem. Phys. Lett.* **1989**, *155*, 572.
- [36] E. Herbst, G. Winnewisser, K. M. T. Yamada, D. J. Defrees, A. D. McLean, *J. Chem. Phys.* **1989**, *91*, 5905.
- [37] G. Winnewisser, M. Winnewisser, W. Gordy, *J. Chem. Phys.* **1968**, *49*, 3465.
- [38] M. L. Senent, Y. G. Smeyers, R. Dominguez-Gomez, A. Arroyo, S. Fernandez-Herrera, *J. Mol. Spectrosc.* **2000**, *203*, 209.
- [39] G. Winnewisser, *Vib. Spectrosc.* **1995**, *8*, 241.
- [40] M. D. Su, A. Willetts, M. J. Bramley, N. C. Handy, *Mol. Phys.* **1991**, *73*, 1209.
- [41] P. Mittler, G. Winnewisser, K. M. T. Yamada, E. Herbst, *J. Mol. Spectrosc.* **1990**, *140*, 259.
- [42] M. Quack, J. Stohner, unpublished manuscript, 1998.

- [43] W. H. Miller, N. C. Handy, J. E. Adams, *J. Chem. Phys.* **1980**, *72*, 99.
- [44] M. Quack, J. Troe, *Ber. Bunsen-Ges. Phys. Chem.* **1974**, *78*, 240.
- [45] M. Quack, J. Troe, Statistical adiabatic channel model, in 'Encyclopedia of Computational Chemistry', Eds. P. Schleyer, A. Allinger, T. Clark, J. Gasteiger, P. A. Kollmann, H. F. Schaefer III, P. Schreiner, Wiley, New York, 1998, *4*, pp. 2708–2726.
- [46] L. Hofacker, *Z. Naturforsch.* **1963**, *18a*, 607.
- [47] D. Luckhaus, *J. Chem. Phys.* **2000**, *113*, 1329.
- [48] J. K. Laerdahl, P. Schwerdtfeger, *Phys. Rev. A* **1999**, *60*, 4439.
- [49] A. Bakasov, R. Berger, T.-K. Ha, M. Quack, to be published.
- [50] M. J. Frisch, G. W. Trucks, H. B. Schlegel, G. E. Scuseria, M. A. Robb, J. R. Cheeseman, V. G. Zakrzewski, J. A. Montgomery, R. E. Stratmann, J. C. Burant, S. Dapprich, J. M. Millam, A. D. Daniels, K. N. Kudin, M. C. Strain, O. Farkas, J. Tomasi, V. Barone, M. Cossi, R. Cammi, B. Mennucci, C. Pomelli, C. Adamo, S. Clifford, J. Ochterski, G. A. Petersson, P. Y. Ayala, Q. Cui, K. Morokuma, D. K. Malick, A. D. Rabuck, K. Raghavachari, J. B. Foresman, J. Cioslowski, J. V. Ortiz, A. G. Baboul, B. B. Stefanov, G. Liu, A. Liashenko, P. Piskorz, I. Komaromi, R. Gomperts, R. L. Martin, D. J. Fox, T. Keith, M. A. Al-Laham, C. Y. Peng, A. Nanayakkara, M. Challacombe, P. M. W. Gill, B. G. Johnson, W. Chen, M. W. Wong, J. L. Andres, C. Gonzalez, M. Head-Gordon, E. S. Replogle, J. A. Pople, GAUSSIAN 98, Rev. 9, Gaussian Inc. Pittsburgh, PA 15106, U.S.A., 1998.
- [51] C. Møller, M. S. Plesset, *Phys. Rev.* **1934**, *46*, 618.
- [52] M. Quack, M. A. Suhm, *J. Chem. Phys.* **1991**, *95*, 28.
- [53] D. Luckhaus, M. Quack, *Chem. Phys. Lett.* **1992**, *190*, 581.
- [54] R. Meyer, *J. Chem. Phys.* **1970**, *52*, 2053.
- [55] P. Mittler, K. M. T. Yamada, G. Winnewisser, M. Birk, *J. Mol. Spectrosc.* **1994**, *164*, 390.
- [56] B. P. Winnewisser, *J. Mol. Spectrosc.* **1970**, *36*, 414.
- [57] B. P. Winnewisser, M. Winnewisser, *Z. Naturforsch., A* **1968**, *23*, 832.
- [58] S. Urban, J. Behrend, K. M. T. Yamada, G. Winnewisser, *J. Mol. Spectrosc.* **1993**, *161*, 511.
- [59] E. Isoniemi, L. Khriachtchev, M. Pettersson, M. Rasanen, *Chem. Phys. Lett.* **1999**, *311*, 47.
- [60] P. A. L. Batchy-Tom, V. I. Tyulin, V. K. Matveev, *Russ. J. Phys. Chem.* **1999**, *73*, 1988.
- [61] J. Koput, *Chem. Phys. Lett.* **1996**, *259*, 146.
- [62] D. W. Lupo, M. Quack, *Chem. Rev.* **1987**, *87*, 181.
- [63] K. v. Puttkamer, M. Quack, *Chem. Phys.* **1989**, *139*, 31.
- [64] F. F. Crim, *Annu. Rev. Phys. Chem.* **1993**, *44*, 397.
- [65] P. Lazzeretti, R. Zanasi, *Chem. Phys. Lett.* **1997**, *279*, 349.
- [66] L. Wiesenfeld, *Mol. Phys.* **1988**, *64*, 739.
- [67] R. Berger, M. Quack, G. S. Tschumper, *Helv. Chim. Acta* **2000**, *83*, 1919.
- [68] R. Berger, M. Quack, *Chem. Phys. Chem.* **2000**, *1*, 57.
- [69] T. Helgaker, H. J. Jensen, P. Jørgenson, J. Olsen, K. Ruud, H. Ågren, T. Andersen, K. L. Bak, V. Bakken, O. Christiansen, P. Dahle, E. K. Dalskov, T. Enevoldsen, B. Fernandez, H. Heiberg, H. Hettema, D. Jonsson, S. Kirpekar, R. Kobayashi, H. Koch, K. V. Mikkelsen, P. Norman, M. J. Packer, T. Saue, P. R. Taylor, O. Vahtras, *Dalton: An electronic structure program*, Release 1.0 ed., 1997.

Received April 12, 2001